ARTICLE

"Ship-in-a-Bottle" Approach to Synthesize Ag@hm-SiO_2 Yolk/Shell Nanospheres

Wei-qiang Li[a], Guo-zhong Wang[a], Guang-hai Li[a,b], Yun-xia Zhang[a]*

a. Key Laboratory of Materials Physics, Centre for Environmental and Energy Nanomaterials and Anhui Key Laboratory of Nanomaterials and Nanotechnology, Institute of Solid State Physics, Hefei Institutes of Physical Science, Chinese Academy of Sciences, Hefei 230031, China
b. School of Chemistry and Materials Science, University of Science and Technology of China, Hefei 230026, China

(Dated: Received on April 1, 2015; Accepted on May 4, 2015)

An effective protocol is presented for the synthesis of Ag@hm-SiO_2 yolk/shell nanostructures (YSNs) via a facile "ship-in-a-bottle" method. TEM observations show that the as-obtained Ag@hm-SiO_2 YSNs have a single silver core in the interior of hollow mesoporous silica (hm-SiO_2) nanospheres, in which the thickness of hm-SiO_2 outer shell is about 14 nm and the silver core has an average size of about 43 nm. And the content of silver in Ag@hm-SiO_2 YSNs is about 10.29% based on the inductively coupled plasma measurement. The as-synthesized Ag@hm-SiO_2 YSNs exhibited significantly enhanced catalytic performance compared with the pure Ag nanoparticles toward the reduction of 4-nitrophenol to 4-aminophenol in the presence of $NaBH_4$.

Key words: Ag@hm-SiO_2, Yolk/shell, Ship-in-a-bottle, Nanoreactor

I. INTRODUCTION

The design and synthesis of noble metal nanoparticles (NPs) have received much attention due to their superior chemical and physical properties compared to bulk metals and a wide variety of applications in hydrogenation, oxidation, photocatalytic reactions, and other fields [1−5]. However, the pristine noble metal NPs are usually unstable and susceptible to aggregate into larger particles in catalytic reactions due to their high surface energy, thus resulting in serious degradation of catalytic activities, even inactivation in the subsequent recycling catalytic reactions, and purification processes [6]. To solve this problem, one of the most effective strategies is to encapsulate noble metal NPs into mesoporous shell to form yolk/shell nanostructures (YSNs) [7]. Compared with common catalysts, the YSNs possess many structure-related advantages: freely movable active metal core, protective mesoporous-shells, high surface-to-volume ratio, rapid mass transfer, low density, and interstitial hollow space [8, 9], which make them a promising platform for various applications in the fields of catalysis [10], lithium-ion batteries [11], drug delivery [12], detection [13], and sensing [14] and so on.

Recently, great efforts have been made to the preparation of YSNs. In most synthetic methods, using hard or soft templating approaches was coated the performed core with single shell or double-shell of different materials, and the YSNs were produced by selectively etching the core or removing the middle shell [15, 16]. The so-called "pre-core/post-shell" methods are effective in formation of YSNs. In contrast, some researchers in this area try to develop new synthetic routes for YSNs through "pre-shell/post-core" or "ship-in-a-bottle" strategy, in which the core is introduced into the preformed hollow mesoporous shells. Hah and coworkers have successfully synthesized the Cu@silica YSNs by reducing Cu^{2+} with hydrazine monohydrate inside hollow silica nanospheres [17]. Cheng *et al.* reported a method of photoreduction to prepare Ag NPs in polypyrrole-chitosan hollow spheres [18]. And Ag@SiO_2 composites are synthesized by a "two solvents" impregnation method [19]. Recently, Qiao's group reported that various metal NPs (*e.g.*, Au, Pt, Pd) were encapsulated and confined in the void of mesoporous organsilica nanorattle (MSN) using impregnation and reduction of adequate metal precursor, and selective alcohols oxidation using Pd@MSN as catalytic nanoreactor shows high conversion (∼100%) and excellent selectivity (∼99%) [20]. But these methods were subjected to some shortcomings, such as tedious assembly procedures, low-efficiency, and consuming-time, there is still a need to push forward novel effective synthetic routes which can continue to progress the process of the "pre-shell/post-core".

In this work, we developed an effective "ship-in-a-bottle" strategy for the fabrication of Ag@hm-SiO_2 yo-

*Author to whom correspondence should be addressed. E-mail: yxzhang@issp.ac.cn

 ©2015 Chinese Physical Society

lk/shell nanostructures (YSNs) by impregnating hollow mesoporous silica nanospheres in a silver nitrate ($AgNO_3$) alcohol solution and transforming Ag^+ into insoluble AgI around the silica shell, followed by a slow reduction process. In the synthetic process, the Ag core is formed inside the *hm*-SiO_2 nanospheres (HMSNs) through the redox reaction between Ag^+ from the slow release of AgI precipitates and hydroquinone. Ag@*hm*-SiO_2 YSNs are highly active in catalytic reactions, because the surface of silver cores has no any protecting ligand in our current system, which is favorable for further improving their performance in catalytic reaction. The nanoreactor of Ag@*hm*-SiO_2 YSNs can be acted as efficient catalysts for the reduction of 4-nitrophenol (4-NP) in the presence of $NaBH_4$ as a model reaction to evaluate its catalytic performance.

II. EXPERIMENTS

A. Chemicals

Tetraethyl orthosilicate (TEOS, 98%), ammonia solution (25%−28%), methanol, ethanol, sodium carbonate, hydroquinone, and hexadecyl trimethyl ammonium bromide (CTAB) were obtained from Sinopharm Chemical Reagent Co. Ltd. Silver nitrate, and sodium iodide was purchased from Tianjin Guangfu Fine Chemical Research Institute. All reagents were used as received without further purification. The water used was purified through a Millipore system.

B. Preparation of the *hm*-SiO_2 nanospheres

Firstly, monodisperse solid silica (*s*-SiO_2) nanospheres were synthesized following a modified Stöber method [21]. Briefly, 6 mL of TEOS was added in the mixture solution of 71.4 mL of ethanol, 10 mL of deionized water, and 3.14 mL of ammonia solution, which was hydrolyzed and condensed for 4 h at 30 °C water bath with magnetic stirring, resulting in the formation of a white silica colloidal suspension. The *s*-SiO_2 particles were centrifugally separated from the suspension and washed with deionized water and ethanol. Secondly, an additional layer SiO_2 with CTAB as pore-making agents was coated on the surface of the pre-prepared *s*-SiO_2 spheres, forming *s*-SiO_2@CTAB/SiO_2 nanostructures. The CTAB (0.2 g) and *s*-SiO_2 (0.2 g) are dispersed in the mixture of 60 mL of ethanol, 5 mL deionized water and 0.4 mL of ammonia solution at 30 °C water bath with magnetic stirring, then a mixture of 0.6 mL of TEOS and 6 mL of ethanol was injected into the reaction medium by the injection pump at speed of 6 mL/h, and then the reaction was continued for another 4 h. Afterwards, *s*-SiO_2@CTAB/SiO_2 were centrifuged with the speed of 10^4 r/min for 5 min and dispered in 50 mL of 0.4 mol/L Na_2CO_3 at 50 °C for 8 h. The as-obtained products were further centrifuged and washed with deionized water and ethanol for several times. Finally, the products were dried at 60 °C and calcined at 550 °C for 6 h to remove the pore-directing agent CTAB to obtain *hm*-SiO_2 nanospheres.

C. Preparation of the Ag@*hm*-SiO_2 YSNs

Typically, 50 mg of *hm*-SiO_2 was dispersed in 35 mL of methanol with ultrasonic bathing for 0.5 h. $AgNO_3$ solution (1 mol/L, 0.5 mL) was then added to the above suspension with violent magnetic stirring, and 5 mL of NaI methanol solution (0.10 mol/L) was injected into the reaction system via the injection pump at the speed of 5 mL/h. After 0.5 h, 5 mL of hydroquinone methanol solution (0.01 mol/L) was injected into the reaction medium by the injection pump at the speed of 2.5 mL/h. The obtained Ag@*hm*-SiO_2 YSNs was collected by centrifugation (1.2×10^4 r/min, 5 min) and washed with deionized water and ethanol for three times, respectively, followed by drying in vacuum at 50 °C overnight. The excess amount of silver precursors outside the *hm*-SiO_2 nanospheres can be easily washed away thus ensuring exclusive loading of precursor inside the *hm*-SiO_2 nanoreactors.

D. Catalytic activity of the as-prepared Ag@*hm*-SiO_2 YSNs

In a typical procedure, 0.1 mL of Ag@*hm*-SiO_2 catalyst (0.5 mg/mL) was added to a quartz cell containing 4-NP (0.02 mmol/L, 0.2 mL), deionized water (2 mL), and $NaBH_4$ aqueous solution (0.1 mol/L, 0.5 mL). The catalytic reaction process was monitored by UV-Vis spectroscopy, in which the peak intensity of nitrophenolate ion at 400 nm decreased gradually and another peak of 4-aminophenol (4-AP) at 300 nm increased accordingly with the prolonging of catalytic reaction. In addition, the color of the reaction system changed from yellowish-green to colorless via naked-eye observation of the reaction solution. As controlled experiment, Ag NPs with similar size was also evaluated the catalytic activity in the reduction reaction of 4-NP, and all the other experimental conditions were the same as the above.

E. Characterization

Field-emission scanning electron microscope (FE-SEM) images were taken on a Sirion 200 with an accelerating voltage of 10 kV, and transmission electron microscope (TEM) images were collected using JEM-2010, operating at 200 kV. N_2 adsorption/desorption isotherms were obtained using an automated gas sorption analyzer (Autosorb-iQ-Cx). The ζ-potential of

DOI:10.1063/1674-0068/28/cjcp1504056 ©2015 Chinese Physical Society

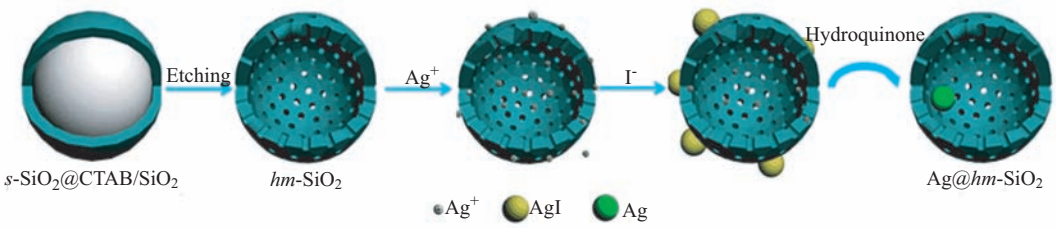

Scheme 1 Schematic representation for the preparation of Ag@*hm*-SiO_2 YSNs.

the *hm*-SiO_2 spheres was tested by Zetasizer 3000SHa. The UV-Vis absorbance spectra were recorded with a Shimadzu UV-3600 spectrophotometer. The contents of Ag NPs in Ag@*hm*-SiO_2 spheres were explored by an Inductively Coupled Plasma Optical Emission Spectrometer (ICP-OES) DUO View spectrometer (Thermo-iCAP 6300). The particle size distribution is measured by using Image J software.

III. RESULTS AND DISCUSSION

The synthetic protocol of Ag@*hm*-SiO_2 YSNs is shown in Scheme 1. In brief, the processes involve the following steps: (i) the synthesis of *s*-SiO_2@CTAB/SiO_2 core/shell structure; (ii) the removal of the *s*-SiO_2 core by hot sodium carbonate solution and the pore-making agent by calcined treatment to form *hm*-SiO_2; (iii) the adsorption of Ag^+ on the surface of *hm*-SiO_2 nanospheres and the following formation of AgI precipitates by reacting with I^-; (iv) the reduction of Ag^+ from the slow release from AgI precipitates by hydroquinone to introduce a single silver core in the void space of *hm*-SiO_2 nanospheres. The preformed *hm*-SiO_2 nanospheres are impregnated in alcohol solution containing $AgNO_3$ for some time to allow Ag^+ to absorb onto their outer surface and further diffuse into the interior of the hollow silica nanospheres. It is reasonable because the ζ-potential of the *hm*-SiO_2 spheres is -15.7 mV in methanol, which makes sure the adsorption of silver ions via the static electronic attraction. When dropping NaI alcohol solution into the reaction system, the Ag^+ transfers to indissoluble AgI precipitates on the surface of the *hm*-SiO_2 nanospheres. After the reduction agent of hydroquinone slowly injects into bulk phase and diffuses into the interior space of *hm*-SiO_2 nanospheres, the Ag^+ ions are reduced to metallic Ag^0 and further grown up into Ag NPs.

SEM and TEM images were employed to investigate the morphology, size, and microstructures of the as-prepared *hm*-SiO_2. The synthesized strategy of *hm*-SiO_2 relies on a self-templating method and a cationic surfactant assisted selective etching strategy [21, 22], in which the mesopores are formed by using CTAB as the pore-directing agent. Figure 1(a) shows the as-prepared *hm*-SiO_2 particles have a smooth spherical morphology with an average diameter of about

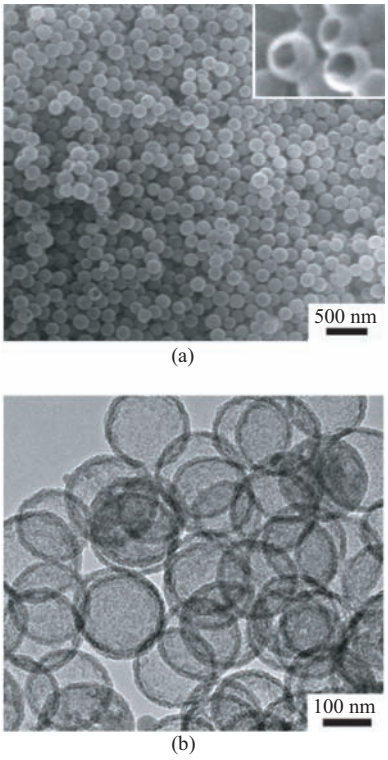

FIG. 1 (a) The SEM image of *hm*-SiO_2 nanospheres. Inset: a typical SEM image of broken *hm*-SiO_2 nanospheres. (b) TEM image of *hm*-SiO_2 nanospheres.

170 nm, and the corresponding inset displays several broken nanospheres, which confirms the hollow structure of the as-prepared nanospheres. In addition, it can be seen from TEM image in Fig.1(b) that the mean shell thickness of SiO_2 hollow spheres is about 14 nm. N_2 adsorption analysis was carried out to characterize the specific surface area and porous structures of the as-prepared *hm*-SiO_2 nanospheres. By the classification of hysteresis loops given by the IUPAC, the IV-type nitrogen absorption-desorption curve (as shown in Fig.2(a)) with a type H3 hysteresis loop exhibits a characteristic of mesoporous materials. And the surface area and total pore volume were calculated to be 171.69 m^2/g and 0.902 cm^3/g, respectively. As revealed by the pore size distribution (shown in Fig.2(b)) obtained from the analysis of the desorption branch of

DOI:10.1063/1674-0068/28/cjcp1504056 ©2015 Chinese Physical Society

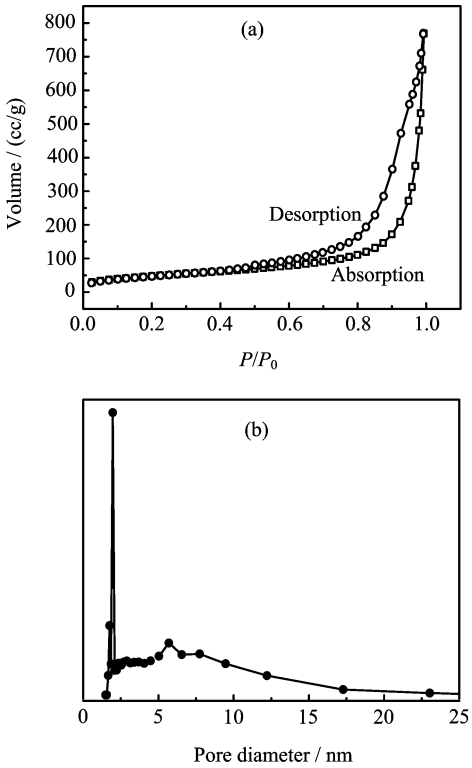

FIG. 2 N_2 absorption-desorption isotherm of (a) the *hm*-SiO_2 nanospheres and (b) the corresponding pore size distributions calculated by the BJH method.

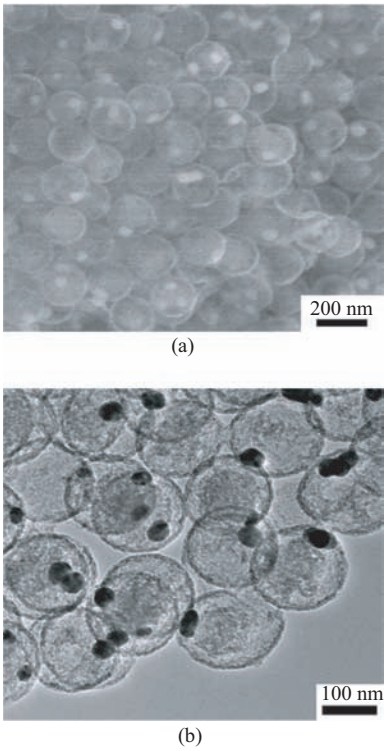

FIG. 3 (a) SEM and (b) TEM images of Ag@*hm*-SiO_2 YSNs.

the isotherm using the Barrett-Joyner-Halenda (BJH) method, we can see that as-prepared *hm*-SiO_2 samples have a rather narrow pore size distribution centered at 1.95 nm, which is originated from CTAB templates. Interestingly, there is another wide mesopore distribution in the range of 4.5 nm to 8 nm, which is not mesoporous within the silica shell but the accumulated pores among *hm*-SiO_2 nanospheres. These pores are randomly distributed over the siliceous shell, which is beneficial to promoting the rapid diffusion of various reactants and products in/out nanoreactor during the process of reaction and enhance the rate of the reaction. After the incorporation of silver cores in the interior of *hm*-SiO_2 nanospheres, the spherical morphology remains unchanged (Fig.3(a)). Figure 3(b) shows the TEM image of the resulting composite particles. The noticeable contrast and large interval between the inner core and outer shell suggests the formation of yolk/shell structures. The Ag particles appear black and SiO_2 nanoshells are light colored in the image because Ag has a higher electron density and allows fewer electrons to transmit. The silver NP core has nearly a uniform size of about 43 nm and the weight of silver is 10.29% through ICP measurement. Those results confirm that the thin shell of HMSNs and Ag@*hm*-SiO_2 were produced by an effective method.

YSNs have been recognized as ideal frameworks to stabilize metal nanoparticle catalysts owing to the structural feature that noble metal cores are isolated by a permeable porous shell and have relatively homogeneous surrounding environments [23, 24]. The 4-NP reduction reaction is a very important reaction, which can generate 4-AP, an important intermediate for the synthesis of many analgesic and antipyretic drugs [25]. On the other hand, 4-NP is a also common organic pollutant in wastewater [26]. 4-NP reduction reaction catalyzed by a catalyst in the presence of $NaBH_4$ is also widely utilized as a model reaction to evaluate the catalyst performance because there are normally no any side reaction, and both the reactant 4-NP and the product 4-AP have characteristic UV absorption peaks, which can be easily monitored using a UV-Vis spectrometer. Here, we explored the reduction of 4-NP as a standard for evaluating the catalytic activity of Ag@*hm*-SiO_2 YSNs. Without the Ag NPs as catalyst, the reduction can't proceed [27], and it's well-known that this reaction is simple and fast in the presence of metallic surfaces. Generally, the 4-NP solution exhibits a strong absorption peak at 317 nm in neutral or acidic conditions. Once the $NaBH_4$ solution was added, the absorption peak of 4-NP changed immediately from 317 nm to 400 nm due to the formation of 4-nitrophenolate ion. When a trace amount of Ag@*hm*-SiO_2 YSNs were added to the mixed solution of 4-NP and $NaBH_4$, and the color of this solution changed from yellowish-green to colorless, indicating the reduction reaction from 4-

DOI:10.1063/1674-0068/28/cjcp1504056 ©2015 Chinese Physical Society

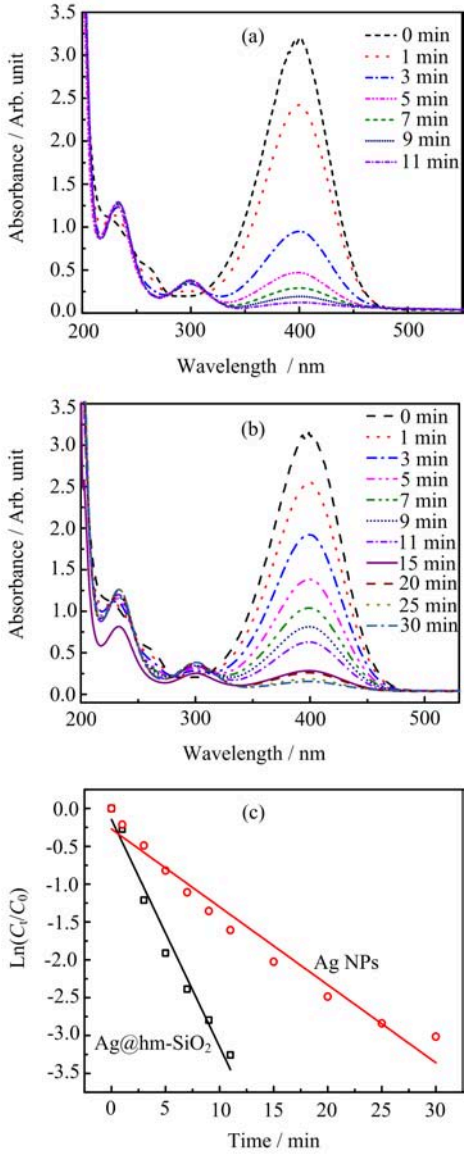

FIG. 4 Time-dependent UV-Vis spectra of 4-NP catalyzed by (a) Ag@*hm*-SiO_2 YSNs, (b) Ag NPs. (c) Plots of $\ln(C_t/C_0)$ versus the reaction time.

NP to 4-AP. As shown in Fig.4(a), the evolution of the UV-Vis spectrum of 4-NP with time upon the addition of Ag@*hm*-SiO_2 YSNs as catalyst, the absorption band of the 4-nitrophenolate ion at 400 nm gradually decreased within 11 min accompanied by a gradual development of a new peak at 300 nm corresponding to the formation of 4-AP, indicating that the $-NO_2$ group of 4-NP had been reduced to the $-NH_2$ group. In a controlled experiment, the catalytic performance Ag NPs with similar sizes was also investigated under the identical condition and the absorbance at 400 nm completely disappears within 30 min (in Fig.4(b)). That's because the Ag NPs gradually form large aggregates with dramatically reduced active surface areas [28]. With respect to the conversion of 4-NP, the catalytic activity is significantly improved for Ag@*hm*-SiO_2 YSNs compared to Ag NPs. Since excess $NaBH_4$ is present in the reaction solution, the reaction can be considered pseudo-first-order with respect to the concentration of 4-NP. By studying the intensity changes at the peak absorbance 400 nm, the rate constant k was determined by a linear plot of $\ln(C_t/C_0)$ and reaction time t, where C_t and C_0 were the concentrations of 4-NP at time t and 0, respectively. As can be seen from the Fig.4(c), the apparent rate constant (k_{app}) can be calculated to be around 0.30 min^{-1} of Ag@*hm*-SiO_2 YSNs and 0.103 min^{-1} of Ag NPs, respectively. These results strongly indicate the improved catalytic activity of Ag@*hm*-SiO_2 YSNs, which is ascribed to the structural advantages: (i) the presence of the porous silica shell is sufficient for stabilizing the catalytic active cores by preventing their aggregation; (ii) the shells are permeable enough so that catalytic surfaces remain accessible to the reactants and products; (iii) the interparticle sintering or aggregation can be efficiently avoided in the single-core/shell structure, which make them remain high activity.

IV. CONCLUSION

In conclusion, Ag@*hm*-SiO_2 yolk/shell nanospheres have been rationally designed and fabricated by using a facile "ship-in-a-bottle" strategy, in which the preformed *hm*-SiO_2 nanospheres was used to the templates allowing effective encapsulation of a single silver core in the interior cavity. The distinctive structural design endows the as-prepared Ag@*hm*-SiO_2 nanoreactors with the excellent catalytic performance towards the reduction of 4-NP in the presence of $NaBH_4$. The synthetic route developed in this work will open new avenues in the design and preparation of other efficient nanoreactors.

V. ACKNOWLEDGMENTS

This work was supported by the National Natural Science Foundation of China (No.51272255, No.51072199, and No.51572263).

[1] D. F. Chen, Z. Y. Han, X. L. Zhou, and L. Z. Gong, Acc. Chem. Res. **47**, 2365 (2014).
[2] S. Han, L. Hu, N. Gao, A. A. Al-Ghamdi, and X. Fang, Adv. Funct. Mater. **24**, 3725 (2014).
[3] M. Rudolph and A. S. Hashmi, Chem. Soc. Rev. **41**, 2448 (2012).
[4] N. R. Shiju and V. V. Guliants, Appl. Catal. A **356**, 1 (2009).
[5] Z. C. Zhang, B. Xu, and X. Wang, Chem. Soc. Rev. **43**, 7870 (2014).

DOI:10.1063/1674-0068/28/cjcp1504056 ©2015 Chinese Physical Society

[6] Y. Dai, Y. Wang, B. Liu, and Y. Yang, Small **11**, 268 (2015).
[7] J. C. Park and H. Song, Nano Res. **4**, 33 (2010).
[8] J. Liu, S. Z. Qiao, J. S. Chen, X. W. Lou, X. Xing, and G. Q. Lu, Chem. Commun. **47**, 12578 (2011).
[9] M. Perez-Lorenzo, B. Vaz, V. Salgueirino, and M. A. Correa-Duarte, Chem. Eur. J. **19**, 12196 (2013).
[10] C. Chen, X. Fang, B. Wu, L. Huang, and N. Zheng, ChemCatChem. **4**, 1578 (2012).
[11] J. Wang, N. Yang, H. Tang, Z. Dong, Q. Jin, M. Yang, D. Kisailus, H. Zhao, Z. Tang, and D. Wang, Angew. Chem. Int. Ed. **52**, 6417 (2013).
[12] L. Zhao, J. Peng, Q. Huang, C. Li, M. Chen, Y. Sun, Q. Lin, L. Zhu, and F. Li, Adv. Funct. Mater. **24**, 363 (2014).
[13] L. Zhou, L. Kuai, W. Li, and B. Geng, ACS Appl. Mater. Interfaces **4**, 6463 (2012).
[14] L. Wang, H. Dou, Z. Lou, and T. Zhang, Nanoscale **5**, 2686 (2013).
[15] B. Liu, W. Zhang, H. Feng, and X. Yang, Chem. Commun. **47**, 11727 (2011).
[16] R. Liu, Y. W. Yeh, V. H. Tam, F. Qu, N. Yao, and R. D. Priestley, Chem. Commun. **50**, 9056 (2014).
[17] H. J. Hah, J. I. Um, S. H. Han, and S. M. Koo, Chem. Commun. **8**, 1012 (2004).
[18] D. Cheng, X. Zhou, H. Xia, and H. S. O. Chan, Chem. Mater. **17**, 3578 (2005).
[19] C. Liu, J. Li, J. Wang, J. Qi, W. Fan, J. Shen, X. Sun, W. Han, and L. Wang, RSC Adv. **5**, 17372 (2015).
[20] J. Liu, H. Q. Yang, F. Kleitz, Z. G. Chen, T. Yang, E. Strounina, G. Q. M. Lu, and S. Z. Qiao, Adv. Funct. Mater. **22**, 591 (2012).
[21] W. Stöber, A. Fink, and E. Bohn, J. Colloid Interface Sci. **26**, 62 (1968).
[22] Z. Teng, S. Wang, X. Su, G. Chen, Y. Liu, Z. Luo, W. Luo, Y. Tang, H. Ju, D. Zhao, and G. Lu, Adv. Mater. **26**, 3741 (2014).
[23] S. Ikeda, S. Ishino, T. Harada, N. Okamoto, T. Sakata, H. Mori, S. Kuwabata, T. Torimoto, and M. Matsumura, Angew. Chem. Int. Ed. **45**, 7063 (2006).
[24] G. Li and Z. Tang, Nanoscale **6**, 3995 (2014).
[25] J. J. Lv, A. J. Wang, X. Ma, R. Y. Xiang, J. R. Chen, and J. J. Feng, J. Mater. Chem. A **3**, 290 (2014).
[26] J. Li, C. Y. Liu, and Y. Liu, J. Mater. Chem. **22**, 8426 (2012).
[27] S. Cao, J. Chen, Y. Ge, L. Fang, Y. Zhang, and A. P. Turner, Chem. Commun. **50**, 118 (2014).
[28] Y. Li, Y. Cao, J. Xie, D. Jia, H. Qin, and Z. Liang, Catal. Commun. **58**, 21 (2015).

DOI:10.1063/1674-0068/28/cjcp1504056 ©2015 Chinese Physical Society